Genetic and physiological insights into the diazotrophic activity of a non-cyanobacterial marine diazotroph

Aurélie Joublin-Delavat[1], Katia Touahri[1,2], Pauline Crétin[1], Amandine Morot[3,4], Sophie Rodrigues[4], Bruno Jesus[5], Florian Trigodet and François Delavat*[,1]

[1] Nantes Université, CNRS, US2B, UMR6286, F-44000 Nantes, France
[2] Laboratoire Chimie et Biochimie de Molécules Bioactives, Université de Strasbourg/CNRS, UMR7177, F-67081 Strasbourg, France
[3] Univ Brest, CNRS, IRD, Ifremer, LEMAR, F-29280 Plouzané, France
[4] Université de Bretagne-Sud, UR3884, LBCM, IUEM, F-56100 Lorient, France
[5] Nantes Université, RSBE[2] ISOMer, UR2160, F-44000 Nantes, France
[6]The University of Chicago, Department of Medicine , Chicago, Illinois, USA
* corresponding author: francois.delavat@univ-nantes.fr

Abstract

Nitrogen (N_2) fixation, or diazotrophy, supports a large part of primary production in oceans. Culture-independent approaches highlighted the presence in abundance of marine non-cyanobacterial diazotrophs (NCD) but their ecophysiology remains elusive, mostly because of the low number of isolated NCD and because of the lack of available genetic tools for these isolates. Here, a dual genetic and functional approach allowed unveiling the ecophysiology of a marine NCD affiliated to the species *Vibrio diazotrophicus*. Physiological characterization of the first marine NCD mutant obtained so far was performed using a soft-gellan assay, demonstrating that a Δ*nifH* mutant in not able to grow in nitrogen-deprived media. Furthermore, we demonstrated that *V. diazotrophicus* produces a thick biofilm under diazotrophic conditions, suggesting biofilm production as an adaptive response of this NCD to cope with the inhibition of nitrogen-fixation by molecular oxygen. Finally, the genomic signature of *V. diazotrophicus* is essentially absent from metagenomic data of *Tara Ocean* expeditions, despite having been isolated from various marine environments. We think that the genetically tractable *V. diazotrophicus* strain used in this study may serve as an ideal model to study the ecophysiology of these overlooked procaryotic group.

Introduction

Nitrogen is a macro-element essential for life, as it is found in many biological molecules (*i.e.* nucleic acids, proteins). The atmosphere is composed by 78% of dinitrogen (N_2) but this form cannot be assimilated by the vast majority of the organisms. The process of N_2 fixation or diazotrophy is pivotal in oceanic ecosystems, since it makes the newly fixed nitrogen accessible to the entire plankton community, fueling primary production (Tang et al., 2019). Diazotrophy is now considered a key player in the biogeochemical cycles of nitrogen, but also of carbon, since it stimulates the biological pump, a mechanism absorbing a significant portion of the carbon dioxide emitted into the atmosphere and exporting it to the ocean seafloor. Diazotrophy is particularly crucial in tropical and subtropical area, where oceanic primary production is typically limited by the limited dissolved inorganic nitrogen (DIN) bioavailability (Capone et al., 2005). In addition, recent *in situ* quantification of N_2 fixation demonstrated high diazotrophic activity in DIN-replete marine environments (Mulholland et al., 2019; Tang et al., 2019), showing the overall importance of diazotrophy in oceans.

Diazotrophy is an anabolic process restricted to some prokaryotic species (found both in *Bacteria* and *Archaea*). *Cyanobacteria* like the free-living *Trichodesmium* are known since decades to be important oceanic nitrogen fixers (Carpenter and Romans, 1991), accounting for at least 1.6 Tmol N in the tropical North Atlantic alone (Capone et al., 2005). Other *Cyanobacteria*, typically living in symbiotic association with photosynthetic microalgae also contribute significantly. These associations include diatom-diazotroph associations (DDA), where filamentous *Cyanobacteria* like *Richelia intracellularis* and *Calothrix rhizosoleniae* can be located either intra- or extracellularly to fix N_2 and transfer the newly fixed nitrogen to sustain diatom growth (Nieves-Morion et al., 2020), receiving organic carbon from its host in return (Foster et al., 2022). DDA associations can account for 0.19 and 0.62 Tmol N per year in Atlantic and Pacific oceans, respectively (Foster et al., 2011). Another example includes the unicellular cyanobacterial lineage UCYN-A, which associate with haptophytes and fixes N_2 even under nitrogen-replete conditions (Mills et al., 2020) and which significantly contribute to N_2 fixation in oceans (Martinez-Perez et al., 2016).

Despite the tremendous data related to cyanobacterial N_2-fixation in oceans, the global N budget in frequently considered unbalanced, as the N loss by denitrification and anammox

70 largely exceeds N input (Landolfi et al., 2018). This suggests that alternative players are
71 missing to equilibrate the N budget. More and more evidence show the presence in all
72 oceans of previously overlooked nitrogen-fixers, not affiliated to the phylum *Cyanobacteria*.
73 Indeed, culture-independent approaches based on the amplification or immunodetection of
74 the *nifH* gene, a gene encoding a subunit of the nitrogenase, conserved among diazotrophs
75 and considered as a biomarker for diazotrophy, have demonstrated the presence of marine
76 Non-Cyanobacterial Diazotrophs (NCDs) (Zehr et al., 1998) in the water column attached to
77 particles (undefined aggregates, faecal pellets) (Farnelid et al., 2019; Geisler et al., 2019) and
78 in deep sea sediments (Kapili et al., 2020). Moreover, *Tara Oceans* expeditions provide
79 metagenomic data from diverse oceanic locations, depths and size fractions, coupled with
80 physical and chemical information (Karsenti et al., 2011; Planes et al., 2019). Analyses of the
81 metagenomes allowed the reconstructions of MAGs (Metagenome-Assembled Genomes)
82 from diverse diazotrophs, including many NCDs, found in abundance in diverse oceans
83 (Delmont et al., 2018; Delmont et al., 2022). Metatranscriptomic analysis from *Tara Oceans*
84 data showed that many NCDs express their *nifH* gene and are therefore active (Delmont et
85 al., 2022).
86 From a biochemical point of view, diazotrophic activity faces a strong metabolic constraint
87 under oxic conditions (Gallon, 1992). Indeed, O_2 acts at different levels to block diazotrophy:
88 it can (i) inhibit the expression of *nif* genes including *nifH* (Hubner et al., 1991; Dixon and
89 Kahn, 2004), (ii) lead to irreversible damages of the nitrogenase (Gallon, 1992), and (iii)
90 reversibly inhibit the nitrogenase activity (Goldberg et al., 1987). This O_2-based inhibition of
91 diazotrophy poses a metabolic conundrum, since many diazotrophs are also aerobes and
92 therefore use O_2 as a terminal electron acceptor for aerobic respiration. To solve this
93 dilemma, terrestrial diazotrophs committed to symbiotic interactions with legume roots
94 (and sometimes on stems (Bonaldi et al., 2011)) are engulfed within a plant organ called
95 nodule. This nodule serves as a physical barrier, limiting O_2 diffusion and creating micro-
96 aerobic environments where both nitrogen fixation and respiration co-occur. Other
97 terrestrial diazotrophs, like the free-living diazotroph *Azotobacter vinelandii* produces a
98 cytochrome *bd* terminal oxidase, that consumes a high volume of O_2, which leads to a rapid
99 decrease in intracellular O_2-tension, allowing nitrogen fixation in overall aerobic
100 environments (Kelly et al., 1990; Poole and Hill, 1997). Additionally, *A. vinelandii* secretes an

101 alginate capsule, which thickness increases with O_2 tension and which serves as a barrier for
102 O_2 diffusion into the cells (Sabra et al., 2000).
103 In addition to the O_2 tension found in oceans, marine *Cyanobacteria* face another challenge
104 when regarding nitrogen fixation, since many of them are photosynthetic and release O_2 as a
105 byproduct of oxygenic photosynthesis. Marine *Cyanobacteria* have therefore also developed
106 various strategies to solve this metabolic constraint. Free-living filamentous *Cyanobacteria*
107 like *Anabaena* sp. (Zhang et al., 2006), but also those living in symbiotic associations with
108 photosynthetic diatoms like *R. intracellularlis* and *C. rhizosoleniae* (Foster et al., 2011)
109 phenotypically differentiate into distinct subpopulations: when DIN becomes limiting, some
110 cells within the filament specialize in nitrogen-fixing factories. These cells, called heterocysts
111 have a modified envelope containing additional layers (a glycolipid and a polysaccharide
112 layer) which restricts O_2 diffusion in the cell cytoplasm (for a review, see (Flores et al.,
113 2019)). Heterocysts commit to a dedicated developmental program (Flores et al., 2019), also
114 marked by the loss of ability to perform oxygenic photosynthesis, which is restricted to the
115 neighboring vegetative cells (Zhang et al., 2006). Molecular exchanges of nitrogen and
116 carbon compounds therefore occur between the vegetative cells and the heterocysts to
117 sustain the growth of the filament (Nieves-Morion et al., 2021). As an alternative to this
118 spatial regulation of diazotrophy, some unicellular *Cyanobacteria* like *Crocosphaera* perform
119 oxygenic photosynthesis during the day and nitrogen fixation during the night (Tuit et al.,
120 2004). Finally, non-heterocyst diazotrophs may protect their nitrogenase from O_2 by the
121 production of hopanoid lipids (Cornejo-Castillo and Zehr, 2019).
122 In contrast, while strategies deployed by marine cyanobacterial diazotrophs to perform
123 nitrogen fixation in oxic environment are documented, knowledge on those for marine NCD
124 remain understudied (Bombar et al., 2016). This knowledge gap is due to the limited number
125 of NCD isolated from marine environments (Farnelid et al., 2014; Martinez-Perez et al.,
126 2018). Additionally, their physiology remains elusive because, to our knowledge, no genetic
127 mutant of marine NCD has been obtained so far, hampering an in-depth physiological
128 characterization of marine NCD.
129 *Vibrio diazotrophicus* is a marine bacterium, firstly isolated from gastrointestinal tract of sea
130 urchins (Guerinot and Patriquin, 1981). It can be found in marine and estuarine
131 environments (Guerinot et al., 1982) as well as in sediments (Castillo et al., 2018) and in
132 enriched marine phytoplankton exometabolites (Fu et al., 2020). The type strain *V.*

133 *diazotrophicus* NS1 (ATCC 33466) was shown by acetylene reduction assay (ARA) to produce
134 nitrogenase and fix N_2 (Guerinot and Patriquin, 1981). The genome of *V. diazotrophicus* NS1
135 is available (accession number BBJY00000000.1, no associated publication or genomic
136 characterization) and other isolates have been fully sequenced (Castillo et al., 2018).
137 However, besides the description of its isolation in 1981 and its taxonomical characterization
138 one year latter (Guerinot et al., 1982), no further physiological or genetic characterization of
139 any member of this species has been performed. Because of its presence in various oceanic
140 environments and because many genetic and molecular tools are available for this genus
141 (Delavat et al., 2018; Morot et al., 2021), we think that *V. diazotrophicus* can constitute an
142 ideal model to assess the ecophysiology of marine NCD and their diazotrophic activity.
143 In this manuscript, we report the physiological description of *V. diazotrophicus* NS1, together
144 with the construction of the first genetic mutant of a marine NCD, impaired in nitrogen-
145 fixation. Importantly, we showed that under nitrogen-deficient conditions, *Vibrio*
146 *diazotrophicus* produces more biofilm, suggesting the role of biofilm as a barrier of O_2
147 diffusion.
148
149 **Material and Methods**
150
151 *Strains and culture conditions*
152 The strains, plasmids and primers used in this study can be found in Table S1, S2 and S3,
153 respectively. Unless otherwise stated, *V. diazotrophicus* NBRC 103148 and *Escherichia coli*
154 were grown in LB at 30°C and 37°C, respectively. The nitrogen-deficient media used in this
155 study is a modified diazotrophic medium for *Vibrio* (MDV), composed similarly to (Guerinot
156 and Patriquin, 1981), with the following modifications: solution 1 was prepared with NaCl
157 0.3 M, $MgSO_4$, $7H_2O$ (0.05 M), $CaCl_2$, $2H_2O$ (0.01 M), KCl (0.01 M), Tris (0.05 M) adjusted to
158 pH 7.5, before the addition of 0.3 $g.l^{-1}$ yeast extract. Solution 2 was prepared in 500 ml H_2O
159 with 0.005 g Na_2MoO_4, $2H_2O$, 40 g glucose, 1 ml of a 3 $g.l^{-1}$ FeNaEDTA,$3H_2O$ stock solution.
160 Solution 3 was prepared in 166 ml H_2O with 0.2 g KH_2PO_4 and 0.8 g K_2HPO_4 adjusted to pH
161 7.2. All 3 solutions were autoclaved, allowed to cool separately, and MDV was prepared by
162 mixing 333 ml of solution 1, 500 ml of solution 2 and 166 ml of solution 3. 1 ml of a vitamin
163 cocktail (stock solution containing 1 $mg.l^{-1}$ biotin, 1 $mg.l^{-1}$ vitamin B12 and 0.2 $g.l^{-1}$ thiamin-
164 HCl) was subsequently added to 1 l MDV.

165 If necessary, trimethoprim (Trim, 10 μg.ml^{-1}), kanamycin (Km, 50 μg.ml^{-1}), diaminopimelic
166 acid (DAP, 0.3 mM), glucose (0.3 g.l^{-1}), L-arabinose (L-ara, 0.2%) or agar (1.5%) were added
167 to the media.
168 Doubling times were determined by spectrophotometry using the TECAN Infinite M1000.
169 Briefly, one colony of each studied strain was inoculated in LB+Trim and incubated
170 overnight. The next morning, cells were washed 3 times to remove old LB from the overnight
171 culture, OD_{600nm} was adjusted to 0.01 with fresh LB, and 200 μl were used to inoculate 4
172 wells from a polystyrene plate (Dutscher, ref 330035). Plate was left in the TECAN
173 instrument set at 30°C without shaking, and OD_{600nm} was measured every 30 minutes for 48
174 hours. Doubling times were calculated from the exponential growth phase of each culture.
175
176 *Strain constructions and DNA techniques*
177 Standard procedures were used for all molecular techniques, following the reagent suppliers
178 recommendations. Deletion of *nifH* was performed by double homologous recombination
179 between a suicide plasmid and the chromosome of *V. diazotrophicus*, following a previously
180 established protocol (Morot et al., 2021), with some adaptations: *V. diazotrophicus* was
181 grown overnight at 30°C (it does not grow at 37°C), cointegrates were incubated in LB+L-ara
182 liquid before plating on LB+L-ara, and the temperature used to incubate the filter-deposited
183 LB+DAP plates was 30°C. The suicide plasmid pFD114 (Table S2) was constructed by
184 amplifying around 750 bp of the upstream and downstream regions of the *nifH* gene of *V.*
185 *diazotrophicus* (BBJY01_570151), using primers 210210 to 210213 (Table S3). Correct
186 deletion of *nifH* was verified using primers 210501 and 210502.
187 Complementation of *nifH* was achieved by amplifying the *nifH* gene and its dedicated
188 promoter, using primers 210204 and 210205 (Table S3). The P_{nifH}-*nifH* amplicon was cloned
189 within the pGEM-T vector (Promega), verified by sequencing and cloned within pFD086
190 (Morot et al., 2021) to replace P_{lac}-*gfp*, using BamHI and XhoI. The resulting pFD120 plasmid
191 was introduced by biparental mating as described above, using β3914 containing pFD120 as
192 a donor strain. All *in silico* plasmid maps are available upon request.
193 Electroporation assays were performed following an already published method (Delavat et
194 al., 2018), except the growing temperature of *V. diazotrophicus*, set at 30°C.
195
196 *Soft-gellan Assay*

197 This medium was prepared as follows (for one tube): 6.7 ml of solution 1 without yeast
198 extract plus 2 mg gellan gum were distributed in 18 cm glass tubes (Dutscher, ref 508232);
199 10 ml of solution 2 containing 3 mg gellan gum in a separate bottle; 3.33 ml of solution 3
200 containing 1 mg gellan gum in a separate bottle. All solutions were autoclaved separately,
201 allowed to cool to 45°C, mixed in the glass tube, gently homogenized by inversion, before
202 the addition of 20 µl of vitamin and Trim. If necessary, 20 µl of NO_3^- (stock solution $NaNO_3$ at
203 46.67 $g.l^{-1}$) were added together with vitamins and Trim after autoclave. If necessary, 20 mg
204 NH_4Cl were added in the 3.33 ml of solution 3 before autoclave.
205 *V. diazotrophicus* containing the empty plasmid pFD085 and *V. diazotrophicus* Δ*nifH*
206 containing either pFD085 or pFD120 were grown overnight in LB+Trim. 1 ml of overnight
207 cultures was subsequently washed with 1 ml nitrogen-free MDV (without yeast extract), and
208 pellets were resuspended with 500 µl nitrogen-free MDV. 100 µl of these washed
209 suspensions were used to inoculate the soft-gellan tubes and tubes closed with a sterile blue
210 rubber stopper, mixed by inversion and before being sealed with an aluminum capsule.
211 Tubes were left for incubation at room temperature for 48 hours. The experiment was
212 performed in triplicates.
213 Dissolved O_2 concentrations were measured with a retractable fiber oxygen microsensor (tip
214 diameter 50-70 µm, OXR50-OI, Pyro Science GmbH, Germany). The oxygen microsensor was
215 connected to a FireSting-O_2 fiber-optic oxygen meter (FireSting-O_2, Pyro Science GmbH,
216 Germany) and signals were recorded with a PC via the software Pyro Oxygen Logger (v3.319,
217 Pyro Science GmbH, Germany). The sensor was linearly calibrated in distilled water by
218 measuring in aerated water (100%) and in the same medium, in which 200 µl of Hcl-cysteine
219 (5 %) was added after media preparation to reduce any trace of O_2 (0%). The position of the
220 sensor was controlled by a micromanipulator (MU1, Pyro Science, GmbH, Germany).
221 Measurements were done before the medium-air interface and at the location of the
222 bacterial ring.
223
224
225 *Biofilm production in microplates*
226 Strains carrying either pFD085 or pFD120 were inoculated from a single colony in 5 ml
227 LB+Trim and incubated overnight at 30°C with shaking. Part of the cultures were washed 3
228 times with LB, diluted to an initial OD_{600nm} of 0.01 with LB+Trim, and 200 µl of this OD-

229 adjusted suspension were inoculated in quadruplicate in a 96-polystyrene-well microplate
230 (Dutscher, ref 330035). The remaining overnight cultures were washed 3 times with MDV,
231 adjusted to an initial OD_{600nm} of 0.01 with MDV+Trim, with MDV+Trim containing 46,67 $mg.l^{-1}$
232 NO_3^- or with MDV+Trim containing 20 $mg.l^{-1}$ NH_4Cl, and 200 µl of these OD-adjusted
233 suspensions were inoculated in quadruplicate in the same microplate. Plates were placed in
234 a microplate reader (TECAN Infinite M1000) for 48 hours at 30°C without shaking, and
235 OD_{600nm} was measured every 30 minutes. After 48 hours, plates were treated following an
236 already established protocol (Morot et al., 2021). Biofilm production was corrected by
237 dividing the OD_{550nm} measured after crystal violet staining by the maximal OD_{600nm} measured
238 during the growing time of the corresponding well.
239
240 *Biofilm production on flowcells*
241 *V. diazotrophicus* biofilms were grown at 30°C under hydrodynamic conditions in a three-
242 channel flow cell (1 x 4 x 44 mm; Biocentrum, DTU, Denmark (Pamp et al., 2009)). The flow
243 system was assembled, prepared and sterilized as described by Tolker-Nielsen and Sternberg
244 (Tolker-Nielsen and Sternberg, 2011). The substratum consisted of a microscope glass
245 coverslip (24 x 50 mm; KnittelGlasser, Braunschweig, Germany). Each channel was
246 inoculated with 250 µl of an overnight LB+Trim culture of *V. diazotrophicus* pFD086 diluted
247 (after 3 washing steps in MDV) to an OD_{600nm} of 0.1 in MDV. A 2h-attachment step was
248 performed without any flow of medium. Then a 5 $ml.h^{-1}$ flow of MDV was applied for 24 h
249 using a Watson Marlow 205U peristaltic pump (Watson Marlow, Falmouth, UK). Biofilms
250 were observed by monitoring the GFP fluorescence with a LSM 710 Confocal Laser Scanning
251 Microscope (Zeiss, Oberkochen, Germany) using a 40x oil immersion objective. GFP was
252 excited at 488 nm and fluorescence emission was detected between 500 and 550 nm.
253 Images were acquired at intervals of 1 µm throughout the whole depth of the biofilm. ZEN
254 2.1 software (Zeiss, Oberkochen, Germany) was used for visualization and image processing.
255 Quantitative analyses of image stacks were performed using COMSTAT software

256 (http://www.imageanalysis.dk/) (Heydorn et al., 2000). Analysis was performed from 3
257 biological replicates (independent experiments) and 8 technical replicates, every replicate
258 comprising 3 to 5 stacked images.
259
260 *Statistical analyses*
261 All statistical analyses were performed using GraphPad Prism; *p* values <0.05 were
262 considered statistically significant.
263
264 Phylogenomics, pangenomics and metagenomics detection of V. diazotrophicus NS1
265 We used anvi'o 7.1 (Eren et al., 2021) and the contigs snakemake (Koster and Rahmann,
266 2018) workflow with the heterotrophic bacterial diazotroph MAGs from Delmont et al.
267 (Delmont et al., 2022). Briefly, the workflow created a contigs database with "anvi-gen-
268 contigs-database," which used Prodigal version 2.6.3 (Hyatt et al., 2010) to identify open
269 reading frames. It used "anvi-run-hmm" to detect the single-copy core genes from bacteria
270 (n = 71, modified from (Lee, 2019)), ribosomal RNAs (rRNAs) (n = 12, modified from
271 https://github.com/tseemann/barrnap). For the phylogenomic tree of *V. diazotrophicus* NS1
272 and the MAGs from (Delmont et al., 2022), we selected 16 bacterial SCGs present in at least
273 40 out of the 41 genomes, which we concatenated and aligned using Muscle v3.8.1551
274 (Edgar, 2004) and used FastTree 2.1.11 (Price et al., 2010) to generate a tree. We used "anvi-
275 interactive" to visualize the phylogenomic tree.
276 To compare *V. diazotrophicus* NS1 with publicly available genomes of the same species, we
277 used "ncbi-genome-download" (https://github.com/kblin/ncbi-genome-download) to get all
278 *V. diazotrophicus* genomes from GenBank. We discarded two genomes for their very small
279 size. We used anvi'o Pangenomics snakemake workflow to compare the gene content
280 between the genomes. The workflow used Prodigal to identify open reading frames,
281 DIAMOND v2.0.14 (Buchfink et al., 2015) to quantify the similarity between each pair of
282 genes, the Markov Clustering Algorithm (MCL) to identify gene clusters, and Muscle
283 v3.8.1551 to align amino acid sequences. We used "anvi-compute-genome-similarity" to
284 compute the Average Nucleotide Identity (ANI) using pyANI v0.2.11 and visualized the
285 pangenome using "anvi-display-pan". We used the "functional homogeneity" index to filter
286 for more divergent gene clusters (max functional homogeneity of 0.95), which we used to

287 generate a *V. diazotrophicus* specific phylogenomic tree (n=99 genes) using the same
288 approach as described above (Muscle v3.8.1551 and FastTree 2.1.11).
289 We used COG20 (Galperin et al., 2021), KOfam (Aramaki et al., 2020) and the InterPro
290 website (Jones et al., 2014) to identify the nitrogen fixation associated genes. We extracted
291 three loci from each genome using "anvi-export-loci" and the anchor genes nifH (K02588),
292 nifU (K02594) and nifQ (K15790) and used the R package "gggenes"
293 (https://wilkox.org/gggenes/) to visualize the gene synteny.
294 We have also used metagenomes from the TARA ocean project to recruit reads on to *V.*
295 *diazotrophicus* NS1. Briefly, we use the "metagenomics" snakemake workflow in anvi'o and
296 mapped metagenomics short-reads using Bowtie2 (Langmead and Salzberg, 2012) and
297 summarized the results with `anvi-summarize`. We used the "detection" value to estimate
298 the presence/absence of V. diazotrophicus NS1 in both the prokaryotic and large size
299 fraction metagenomes.
300
301
302 **Results**
303
304 *Optimization of genetic tools for V. diazotrophicus NS1*
305
306 *V. diazotrophicus* NS1 is a marine strain, for which no genetic mutant has been described.
307 Because this strain might serve as an ideal model for genetic and ecophysiological
308 characterization of marine NCD, we sought to develop and optimize a genetic protocol for *V.*
309 *diazotrophicus* NS1. To achieve this aim, we first applied and modified an electroporation
310 protocol, originally developed for *Vibrio harveyi* and *Pseudoalteromonas* sp. (Delavat et al.,
311 2018). We tested different variants of the protocol, by using either 1- or 2 mm
312 electroporation cuvettes, modifying the voltage from 1500 to 2500 V in the presence or
313 absence of 15% glycerol in the sucrose buffer (Delavat et al., 2018), from stationary-phase
314 cultures grown in LB or LBS at 30°C. The best electroporation protocol yielded 81 CFU/μg
315 DNA, and was obtained when the following protocol was applied: glycerol-containing buffer
316 was used to wash LB-grown cultures, and the electroporation voltage was set at 2000 V in a
317 2 mm electroporation cuvette (data not shown). This demonstrates that, although being at
318 low efficiency, electroporation can be applied for this strain.

319 In order to improve the efficiency of exogenous DNA transfer to *V. diazotrophicus* NS1, we
320 also performed bi- and triparental mating as recently developed (Morot et al., 2021). Both
321 conjugations were successful for transferring the replicative plasmid pFD086 to *V.*
322 *diazotrophicus* NS1, giving rise to bright GFP-fluorescent cells (Figure 1). Finally, applying this
323 protocol, we successfully inserted a mini-Tn7 in *V. diazotrophicus* NS1 containing the
324 unstable pFD052 plasmid expressing the Tn7-transposase (Delavat et al., 2018), the latter
325 being subsequently cured (data not shown).
326
327 *Construction of a nifH deletion mutant and physiological characterization*
328
329 Unveiling the genetics and ecophysiology underlying diazotrophy in *V. diazotrophicus*
330 requires the deletion of genes and the subsequent physiological characterization of the
331 obtained mutants. In this study we focused on the deletion of the *nifH* gene
332 (BBJY01_570151), applying an adapted protocol successfully used for *V. harveyi* ORM4
333 (Morot et al., 2021). Using this protocol, a clean *nifH* deletion mutant was obtained (Figure
334 2A). This mutant does not show any growth phenotype when growing in LB-rich medium
335 (Figure 2B).
336 In order to characterize the diazotrophic activity of the *nifH* mutant, we developed a soft-
337 gellan assay, characterized by the use of a nitrogen-deprived medium containing 0.3% gellan
338 gum. Inoculating tubes sealed with a blue rubber stopper and an aluminum capsule (Figure
339 3) with *V. diazotrophicus* NS1 containing the empty plasmid pFD085 led to a growth of this
340 strain throughout the entire tube height (with a higher biomass closer to the surface) when
341 NH_4^+ is added. Importantly, in the absence of NH_4^+, a single ring is visible after 48h, located
342 around 15 mm below the surface of the medium. Applying this assay for the *nifH* mutant
343 containing pFD085 gave a similar pattern as the one of the wild type when grown with NH_4^+.
344 However, in the complete absence of nitrogen, no band nor growth was detectable in the
345 *nifH* mutant. Additionally, no band was visible when tubes were left for 2 more weeks,
346 indicating that the observed phenotype does not correspond to a longer lag phase in this
347 medium. *In trans* complementation of the *nifH* deletion mutant by the introduction by
348 conjugation of a replicative plasmid containing the entire *nifH* gene and its P_{nifH} promoter
349 restored the wild type phenotype, with the formation of a clear band located roughly 15 mm
350 below the surface of the medium (Figure 3). We subsequently repeated the experiment,

351 using NO_3^- as an alternative bioavailable nitrogen source, and the results were identical (see
352 Figure S1). Thus, we demonstrated that growth of *V. diazotrophicus* NS1 under nitrogen-
353 deprived medium is dependent on an intact nitrogenase.
354 The O_2 concentration in the soft-gellan tube was subsequently measured in the headspace
355 and at the location (or corresponding depth) of the growing ring. Uninoculated soft-gellan
356 tubes showed a high O_2 concentration at both locations, with values ranging from 173.6 μM
357 (sd 20.1) at a depth corresponding to the growing ring to 245.5 μM (sd 1.9) in the head
358 space. In contrast, after 72 hours growth of *V. diazotrophicus* in nitrogen-free MDV, the O_2
359 decreased to a concentration of 1.6 μM (sd 1.1) at the location of the ring, while this
360 concentration was 238.8 μM (sd 1.4) in the headspace. To better approximate the O_2
361 concentration at a depth where N_2 fixation can occur, we quantified this concentration in 12
362 hours-inoculated tubes, where the growing ring is not yet formed. Under this condition, a O_2
363 concentration of 14.8 μM (sd 7.7) is quantified at a similar depth as the one where the ring
364 will form 2 days later. Thus, we demonstrated here that diazotrophy occurs under
365 microaerobic conditions. Moreover, a subsequent soft-gellan experiment using *V.*
366 *diazotrophicus* NS1 constitutively expressing GFP (thanks to the pFD086 plasmid it contains)
367 showed that cells growing under microaerobic conditions within the ring are free-living and
368 isolated, and don't form aggregates (Figure S2).
369
370 *V. diazotrophicus* produces more biofilm in MDV
371
372 In order to determine the possible regulatory mechanism deployed by *V. diazotrophicus* NS1
373 to avoid the nitrogenase inhibition by O_2, we sought to quantify the ability of this strain to
374 produce biofilm. Microplates containing either LB, MDV or MDV supplemented with either
375 NO_3^- or NH_4^+, plus trimethoprim were inoculated with either *V. diazotrophicus* NS1 (pFD085),
376 *V. diazotrophicus* NS1 Δ*nifH* (pFD085) or *V. diazotrophicus* NS1 Δ*nifH* (pFD120), and left
377 without shaking at 30°C. Neither *V. diazotrophicus* NS1 nor their derivatives do produce any
378 biofilm when grown in LB. However, when grown in MDV, biofilm production significantly
379 increased in the three tested strains (Figure 4A), and this biofilm was located at the bottom
380 of the wells. Of note, the original MDV used for this experiment contains 100 $mg.l^{-1}$ yeast
381 extract, which provides low-but-necessary bioavailable nitrogen for the *nifH* mutant to grow,
382 allowing direct comparison of the 3 tested strains. Importantly, when MDV was

383 supplemented with NO_3^- or NH_4^+, the biofilm production significantly decreased as
384 compared to the one obtained in MDV medium. Additionally, we observed only subtle
385 differences between the different tested strains, all three of them producing more biofilm in
386 MDV as compared to LB and to MDV supplemented with either NO_3^- or NH_4^+. This increase in
387 biofilm formation in MDV suggests that in a nitrogen-limited medium, the production of
388 biofilm by *V. diazotrophicus* NS1 might protect its nitrogenase from an excess in O_2.
389 Furthermore, the thickness and biovolume of the biofilm produced in MDV by *V.*
390 *diazotrophicus* were quantified by confocal microscopy, using flow cells. Under this
391 condition, *V. diazotrophicus* produced an important biofilm (average biovolume of 11.70
392 $\mu m^3.\mu m^{-2}$, Standard Error of the Mean SEM 1.64 μm). The thickness of the biofilm was also
393 measured, reaching on average 26.65 μm (SEM 3.25 μm) and a maximal thickness of 46.35
394 μm (SEM 3.34 μm) after 24 hours (Figure 4BCD). After 48 hours, these values increased even
395 more, but the biofilm matrix was too dense and too heterogeneous, probably because of the
396 maturation of the biofilm, causing early dispersal (Supplementary Figure S3).
397
398 *V. diazotrophicus is different from recently discovered heterotrophic bacterial diazotrophs*
399
400 The genome of *V. diazotrophicus* NS1 was compared with the 40 Metagenome-Assembled
401 Genomes (MAGs) of HBDs recently retrieved from *Tara ocean* metagenomes (Delmont et al.,
402 2022). Expectedly, *V. diazotrophicus* NS1 falls in a group containing all MAGs affiliated to
403 *Gammaproteobacteria* (Figure 5A). However, the closest MAG (called HBD_Gamma_02 here
404 and in (Delmont et al., 2022)) seems to be affiliated to the order *Pseudomonales* and not to
405 *Vibrionales*, and ANI comparison (value of 0.68, see Table S4) confirmed their phylogenomic
406 distance. In addition, the genome of V. diazotrophicus NS1 was not detected in the Tara
407 ocean metagenomes (max detection was 8% of the genome, Table S5). We subsequently
408 compared the genomic relatedness of *V. diazotrophicus* NS1 to the genomes of 6 strains
409 isolated from deep subsurface sediments of the Baltic Sea (Castillo et al., 2018), to the one
410 isolated from phytoplankton exometabolite-enrichments (Fu et al., 2020) and to strain *V.*
411 *diazotrophicus* 99A isolated in Pennsylvania (unpublished data). Pangenomic and
412 phylogenomic analyses showed that *V. diazotrophicus* NS1 is closely related to 6 of these 8
413 strains (Figure 5B), with *V. diazotrophicus* 60.6B and HF9B standing a bit apart, possibly
414 belonging to a new species (ANIb comparison below 0.95, see Figure 5B and Table S4). Of

415 note, all of these nine *V. diazotrophicus* isolates carry a single copy of the *nifH* gene (Figure
416 5B and 5C) and a similar *nif* cluster (Figure 5C).
417
418 **Discussion**
419
420 Nitrogen fixation is a major metabolism in many ecosystems, supplying living micro- and
421 macro-organisms with otherwise scarce bioavailable nitrogen. In oceans, diazotrophy can
422 account for half of the annual new production in euphotic zones in oligotrophic oceans (Karl
423 et al., 1997). The diversity of marine diazotrophs has long been thought to be restricted to
424 members of the phylum *Cyanobacteria*. However, culture-independent approaches, like
425 those targeting the *nifH* gene or metagenomic and metatranscriptomic analyses from
426 various oceanic samples demonstrated the presence in abundance of non-cyanobacterial
427 diazotrophs (NCD, (Zehr et al., 1998; Delmont et al., 2018; Farnelid et al., 2019; Geisler et al.,
428 2019; Kapili et al., 2020; Delmont et al., 2022)). Despite these observations, few marine NCD
429 have been brought to culture (Farnelid et al., 2014; Martinez-Perez et al., 2018), hampering
430 in depth understanding of their ecophysiology and contribution to global N budget in
431 oceans. The goal of this study was to unveil the physiology of *V. diazotrophicus* NS1, a
432 marine NCD isolated already 40 years ago (Guerinot and Patriquin, 1981) but surprisingly
433 overlooked for in-depth analysis of its physiology.
434 The genome of *V. diazotrophicus* NS1 is available, and its analysis shows that it contains one
435 *nif* cluster, separated in 3 chromosomal locations and spanning some 110 Kbp (Figure 5C).
436 This cluster is found in all *V. diazotrophicus* strains whose genomes have been sequenced,
437 with only minor differences. The presence of only one *nif* cluster is unlike other soil NCD like
438 those belonging to the *Bradyrhizobium* genus, which can be endowed with 2 *nif* clusters (de
439 Matos et al., 2021). In line with this observation, we showed here that the *nifH* gene of all
440 sequenced *V. diazotrophicus* strains is part of the single-copy core gene fraction of the
441 genome (Figure 5C), unlike many other *Bradyrhizobium* strains (de Matos et al., 2021).
442 Because *V. diazotrophicus* NS1 belongs to one of the few marine NCD isolated, we sought to
443 develop and optimize genetic and molecular tools for this strain. Results show that *V.*
444 *diazotrophicus* is genetically tractable, both by electroporation and conjugation.
445 Electroporation efficiency was albeit low, as compared to the one reported for other *Vibrio*
446 or *Pseudoalteromonas* species (Delavat et al., 2018). Improving the electroporation

447 efficiency will require trials and errors, but having an already functional method reinforce its
448 high potential for rapid introduction of exogenous DNA, strengthened by its functionality in
449 other marine bacteria like *Algoriphagus machipongonensis* (Xu et al., 2022) or human
450 pathogens like *Vibrio parahaemolyticus* (Soree et al., 2022). Conjugation was more efficient,
451 both for the transfer of replicative plasmids and for the insertion of mini-transposons.
452 Mating is however more time-consuming and requires efficient counter-selection of the
453 donor. This counterselection is achieved here thanks to the use of strain β3914 (Le Roux et
454 al., 2007), a RP4+ and DAP-auxotroph strain, and thanks to a protocol recently optimized for
455 other *Vibrio* species (Morot et al., 2021).
456 In order to study the ecophysiology of marine NCD, we next focused on the targeted
457 deletion of genes. The *nifH* was the ideal candidate for gene deletion since it is found in only
458 one copy in *V. diazotrophicus* NS1, it is conserved in diazotrophs and considered as a
459 biomarker for diazotrophy and it codes the nitrogenase-reductase, and essential component
460 of the nitrogenase multiprotein complex. Adapting an already existing protocol (Morot et al.,
461 2021), we were able to perform a scarless deletion of the *nifH* gene in this strain. To our
462 knowledge, this mutant represents the first marine NCD mutant described in literature,
463 opening an avenue for a better characterization of their ecophysiology and role in the N and
464 C biogeochemical cycles. Its nitrogen-fixation capability was subsequently tested thanks to a
465 strain- and medium-adapted soft-gellan bioassay (Hashidoko et al., 2002; Hara et al., 2009).
466 This soft-gellan assay allows the inoculated bacteria to "find" their best appropriate O_2-
467 tension for optimized growth, characterized by a visible ring formed within the semi-solid
468 medium (Hashidoko et al., 2002). When nitrogen-free medium is used, the location of this
469 growing ring corresponds to the delicate balance between O_2 tension -necessary for aerobic
470 respiration- and diazotrophy inhibition by O_2. Additionally, gellan gum allows a complete
471 transparency of the medium and better visualization of bacterial growth (Hashidoko et al.,
472 2002), frequently allows faster growth and a higher bacterial diversity recovered (Tamaki et
473 al., 2009; Delavat et al., 2012; Delavat et al., 2013) and, importantly, bacteria grown in soft-
474 gellan show a much higher diazotrophic activity compared to the same bacteria grown in
475 soft-agar (Hara et al., 2009).
476 When grown in a nitrogen-free soft-gellan medium, we clearly showed that, unlike *V.*
477 *diazotrophicus* NS1 wild type, the Δ*nifH* mutant is unable to grow, while supplementing the
478 medium with NO_3^- or NH_4^+ as an organic nitrogen source allows its growth (Figure 3 and

479 Figure S1). Moreover, *in trans* complementation of the *nifH* mutant restores its capacity to
480 grow in a nitrogen-free medium, demonstrating that growth in this medium is dependent on
481 an intact nitrogenase. We also show here that the developed soft-gellan bioassay is powerful
482 to screen for diazotrophic activity and to phenotypically differentiate *V. diazotrophicus*
483 mutants, *e.g.* those related to N_2 fixation (catalytic or regulatory genes) or related to
484 protection from O_2. This experiment and the fact that no growth was obtained in the Δ*nifH*
485 mutant even after prolonged incubation in this soft-gellan tubes also confirm the presence
486 of only one copy of the *nifH* gene in the genome *V. diazotrophicus* NS1 and no paralog being
487 able to partially complement this mutation (Figure 5B).
488
489 Because of the inhibition of diazotrophy by O_2, nitrogen-fixation occurs at intermediate O_2
490 tension. We demonstrated here with a nitrogen-free soft-gellan medium that *V.*
491 *diazotrophicus* NS1 grows under microoxic conditions, ranging from 1 to 15 μM O_2 to
492 achieve a sufficient N_2 fixation activity to sustain its growth (Figure 3). Decreasing the local
493 O_2 tension is therefore important, and can be achieved by different means (for a review, see
494 (Gallon, 1992). As the ecophysiology of marine NCD is basically unknown, we tested whether
495 *V. diazotrophicus* NS1 is able to produce a biofilm, which would restrict the diffusion of O_2 in
496 the cells. Indeed, this strain produces more biofilm when grown in a nitrogen-limited
497 medium, compared with the biofilm formed in LB-rich medium (Figure 4A). This biofilm
498 formation decreases when NO_3^- or NH_4^+ is added as an alternative bioavailable nitrogen
499 source. These results were similar for the Δ*nifH* mutant and the Δ*nifH* complemented strain
500 (Figure 4A), demonstrating that biofilm production is not dependent on the presence of an
501 intact nitrogenase and that both processes are genetically decoupled, at least at this genetic
502 hierarchy. The thickness of the biofilm was quantified using flow cells, showing that *V.*
503 *diazotrophicus* NS1 produces a substantial biofilm after 24 hours of growth (Figure 4BCD).
504 The thickness of the biofilm measured in this experiment (on average of 26.65 μm) probably
505 serves as a barrier for O_2-diffusion. Indeed, this value is coherent with previous data,
506 showing the rapid decrease in O_2 in thick biofilms, which ultimately turn anoxic (Stewart et
507 al., 2016). Thus, *V. diazotrophicus* NS1 produces biofilm when grown under nitrogen-limited
508 condition, which might restrict O_2 diffusion, thus help solving the dilemma of nitrogenase
509 inhibition by O_2. This behaviour is analog to the one of the terrestrial strain *Pseudomonas*
510 *stutzeri* A1501, which produces biofilm under nitrogen-starved conditions (Wang et al.,

511 2017). Marine non cyanobacterial diazotrophs are in contrast less studied. Cell aggregates of
512 1-4 mm in diameter were observed for the marine diazotroph *P. stutzeri* BAL361 when
513 grown in nitrogen-free media under oxic condition, which was hypothesized to be an
514 adaptive mechanism for *P. stutzeri* BAL361 to fix N_2 despite high surrounding O_2-tension
515 (Bentzon-Tilia et al., 2015). Cell aggregation and exopolysaccharide production is also
516 suspected to play a role in the diazotrophic activity of the marine NCD *Sagittula castanea*,
517 even though cell aggregation was also observed under anoxic conditions in this strain
518 (Martinez-Perez et al., 2018). In this study, we showed that *V. diazotrophicus* cells grown
519 under microaerobic conditions in nitrogen-free media don't form aggregates (Figure S2), and
520 demonstrated an increase in biofilm density and biofilm thickness of a marine NCD when
521 grown under nitrogen-limited conditions as compared to LB-grown culture, constituting an
522 additional level of evidence that biofilm formation is important for these bacteria when
523 grown under oxic condition. This hypothesis is reinforced by the recent demonstration of the
524 high prevalence of marine NCD in high size fractions of marine metagenomic samples
525 (Delmont et al., 2022), suggesting NCD aggregation on particles and planktonic aggregates
526 (Farnelid et al., 2019; Geisler et al., 2019).
527 *V. diazotrophicus* is a bacterial species which has been isolated from different marine
528 environments, including sea water (Guerinot et al., 1982), gastrointestinal tractus of sea
529 urchin (Guerinot and Patriquin, 1981) or deep see sediments (Castillo et al., 2018), and from
530 enriched-phytoplankton exometabolites (Fu et al., 2020). However, this species is barely
531 detected from metagenomes coming from *Tara ocean* expeditions (Table S5), and is only
532 distantly related to newly discovered MAGs (Delmont et al., 2022). This almost absent
533 distribution from those metagenomic samples despite their effective presence in various
534 marine environments suggests that additional NCD live in alternative ecological niches that
535 have been overlooked by most metagenomic studies, like those from macroorganisms (*e.g.*
536 see urchins) or those from deep see sediment (Castillo et al., 2018).
537 In conclusion, this study allowed unveiling the ecophysiology of a marine NCD belonging to
538 the species *V. diazotrophicus*, which might serve as an ideal model to decipher their
539 ecological importance related to the N and C biogeochemical cycles and their genetic and
540 physiological adaptations to their environments, including the O_2-tension and the presence
541 of dissolved inorganic nitrogen.
542

Acknowledgments

The authors would like to thank Corentin Ramaugé-Parra for his help in the initial optimization of the genetic tools. The authors acknowledge the MicroScope plateform (https://mage.genoscope.cns.fr/microscope/home/index.php) for providing access to their plateform. This work was supported by the "Connect Talent" EpiAlg project awarded to Leila Tirichine, and by the "Rising Star" SMIDIDI project awarded to François Delavat, both from the French Pays de la Loire Region.

References

Aramaki, T., Blanc-Mathieu, R., Endo, H., Ohkubo, K., Kanehisa, M., Goto, S., and Ogata, H. (2020) KofamKOALA: KEGG Ortholog assignment based on profile HMM and adaptive score threshold. *Bioinformatics* **36**: 2251-2252.

Bentzon-Tilia, M., Severin, I., Hansen, L.H., and Riemann, L. (2015) Genomics and Ecophysiology of Heterotrophic Nitrogen-Fixing Bacteria Isolated from Estuarine Surface Water. *mBio* **6**: e00929.

Bombar, D., Paerl, R.W., and Riemann, L. (2016) Marine non-cyanobacterial diazotrophs: moving beyond molecular detection. *Trends Microbiol* **24**: 916-927.

Bonaldi, K., Gargani, D., Prin, Y., Fardoux, J., Gully, D., Nouwen, N. et al. (2011) Nodulation of *Aeschynomene afraspera* and *A. indica* by Photosynthetic *Bradyrhizobium* sp. Strain ORS285: The Nod-Dependent Versus the Nod-Independent Symbiotic Interaction. *Mol Plant-Microbe Interact* **24**: 1359-1371.

Buchfink, B., Xie, C., and Huson, D.H. (2015) Fast and sensitive protein alignment using DIAMOND. *Nat Methods* **12**: 59-60.

Capone, D.G., Burns, J.A., Montoya, J.P., Subramaniam, A., Mahaffey, C., Gunderson, T. et al. (2005) Nitrogen fixation by *Trichodesmium* spp.: An important source of new nitrogen to the tropical and subtropical North Atlantic Ocean. *Global Biogeochem Cycles* **19**: 1-17.

Carpenter, E.J., and Romans, K. (1991) Major role of the cyanobacterium *Trichodesmium* in nutrient cycling in the north atlantic ocean. *Science* **254**: 1356-1358.

Castillo, D., Vandieken, V., Engelen, B., Engelhardt, T., and Middelboe, M. (2018) Draft genome sequences of six *Vibrio diazotrophicus* strains isolated from deep subsurface Ssdiments of the Baltic Sea. *Genome Announc* **6**.

Cornejo-Castillo, F.M., and Zehr, J.P. (2019) Hopanoid lipids may facilitate aerobic nitrogen fixation in the ocean. *Proc Natl Acad Sci U S A* **116**: 18269-18271.

de Matos, G.F., Rouws, L.F.M., Simoes-Araujo, J.L., and Baldani, J.I. (2021) Evolution and function of nitrogen fixation gene clusters in sugarcane associated *Bradyrhizobium* strains. *Environ Microbiol*. **23**: 6148-6162.

Delavat, F., Lett, M.C., and Lièvremont, D. (2012) Novel and unexpected bacterial diversity in an arsenic-rich ecosystem revealed by culture-dependent approaches. *Biol Direct* **7**: art. 28.

Delavat, F., Lett, M.C., and Lievremont, D. (2013) Yeast and bacterial diversity along a transect in an acidic, As-Fe rich environment revealed by cultural approaches. *Sci Tot Environ* **463**: 823-828.

585 Delavat, F., Bidault, A., Pichereau, V., and Paillard, C. (2018) Rapid and efficient protocol to
586 introduce exogenous DNA in *Vibrio harveyi* and *Pseudoalteromonas* sp. *J Microbiol Methods*
587 **154**: 1-5.
588 Delmont, T.O., Quince, C., Shaiber, A., Esen, O.C., Lee, S.T., Rappe, M.S. et al. (2018)
589 Nitrogen-fixing populations of *Planctomycetes* and *Proteobacteria* are abundant in surface
590 ocean metagenomes. *Nat Microbiol* **3**: 804-813.
591 Delmont, T.O., Pierella Karlusich, J.J., Veseli, I., Fuessel, J., Eren, A.M., Foster, R.A. et al.
592 (2022) Heterotrophic bacterial diazotrophs are more abundant than their cyanobacterial
593 counterparts in metagenomes covering most of the sunlit ocean. *ISME J* **16**: 927-936.
594 Dixon, R., and Kahn, D. (2004) Genetic regulation of biological nitrogen fixation. *Nat Rev*
595 *Microbiol* **2**: 621-631.
596 Edgar, R.C. (2004) MUSCLE: multiple sequence alignment with high accuracy and high
597 throughput. *Nucleic Acids Res* **32**: 1792-1797.
598 Eren, A.M., Kiefl, E., Shaiber, A., Veseli, I., Miller, S.E., Schechter, M.S. et al. (2021)
599 Community-led, integrated, reproducible multi-omics with anvi'o. *Nat Microbiol* **6**: 3-6.
600 Farnelid, H., Harder, J., Bentzon-Tilia, M., and Riemann, L. (2014) Isolation of heterotrophic
601 diazotrophic bacteria from estuarine surface waters. *Environ Microbiol* **16**: 3072-3082.
602 Farnelid, H., Turk-Kubo, K., Ploug, H., Ossolinski, J.E., Collins, J.R., van Mooy, B.A.S., and Zehr,
603 J.P. (2019) Diverse diazotrophs are present on sinking particles in the North Pacific
604 Subtropical Gyre. *ISME J* **13**: 170-182.
605 Flores, E., Picossi, S., Valladares, A., and Herrero, A. (2019) Transcriptional regulation of
606 development in heterocyst-forming cyanobacteria. *Biochim Biophys Acta Gene Regul Mech*
607 **1862**: 673-684.
608 Foster, R.A., Kuypers, M.M., Vagner, T., Paerl, R.W., Musat, N., and Zehr, J.P. (2011) Nitrogen
609 fixation and transfer in open ocean diatom-cyanobacterial symbioses. *ISME J* **5**: 1484-1493.
610 Foster, R.A., Tienken, D., Littmann, S., Whitehouse, M.J., Kuypers, M.M.M., and White, A.E.
611 (2022) The rate and fate of N_2 and C fixation by marine diatom-diazotroph symbioses. *ISME J*
612 **16**: 477-487.
613 Fu, H., Smith, C.B., Sharma, S., and Moran, M.A. (2020) Genome Sequences and
614 Metagenome-Assembled Genome Sequences of Microbial Communities Enriched on
615 Phytoplankton Exometabolites. *Microbiol Resour Announc* **9**.
616 Gallon, J.R. (1992) Reconciling the Incompatible - N_2 Fixation and O_2. *New Phytol* **122**: 571-
617 609.
618 Galperin, M.Y., Wolf, Y.I., Makarova, K.S., Vera Alvarez, R., Landsman, D., and Koonin, E.V.
619 (2021) COG database update: focus on microbial diversity, model organisms, and
620 widespread pathogens. *Nucleic Acids Res* **49**: D274-D281.
621 Geisler, E., Bogler, A., Rahav, E., and Bar-Zeev, E. (2019) Direct detection of heterotrophic
622 diazotrophs associated with planktonic aggregates. *Sci Rep* **9**: 9288.
623 Goldberg, I., Nadler, V., and Hochman, A. (1987) Mechanism of nitrogenase switch-off by
624 oxygen. *J Bacteriol* **169**: 874-879.
625 Guerinot, M.L., and Patriquin, D.G. (1981) N_2-fixing vibrios isolated from the gastrointestinal
626 tract of sea urchins. *Can J Microbiol* **27**: 311-317.
627 Guerinot, M.L., West, P.A., Lee, J.V., and Colwell, R.R. (1982) *Vibrio diazotrophicus* sp. nov., a
628 marine nitrogen-fixing bacterium. *Int J Syst Bacteriol* **32**: 350-357.
629 Hara, S., Hashidoko, Y., Desyatkin, R.V., Hatano, R., and Tahara, S. (2009) High rate of N_2
630 fixation by east Siberian cryophilic soil bacteria as determined by measuring acetylene

631 reduction in nitrogen-poor medium solidified with gellan gum. *Appl Environ Microbiol* **75**:
632 2811-2819.
633 Hashidoko, Y., Tada, M., Osaki, M., and Tahara, S. (2002) Soft gel medium solidified with
634 gellan gum for preliminary screening for root-associating, free-living nitrogen-fixing bacteria
635 inhabiting the rhizoplane of plants. *Biosci Biotechnol Biochem* **66**: 2259-2263.
636 Heydorn, A., Nielsen, A.T., Hentzer, M., Sternberg, C., Givskov, M., Ersboll, B.K., and Molin, S.
637 (2000) Quantification of biofilm structures by the novel computer program COMSTAT.
638 *Microbiology-Sgm* **146**: 2395-2407.
639 Hubner, P., Willison, J.C., Vignais, P.M., and Bickle, T.A. (1991) Expression of regulatory *nif*
640 genes in *Rhodobacter capsulatus*. *J Bacteriol* **173**: 2993-2999.
641 Hyatt, D., Chen, G.L., Locascio, P.F., Land, M.L., Larimer, F.W., and Hauser, L.J. (2010)
642 Prodigal: prokaryotic gene recognition and translation initiation site identification. *BMC*
643 *Bioinform* **11**: 119.
644 Jones, P., Binns, D., Chang, H.Y., Fraser, M., Li, W., McAnulla, C. et al. (2014) InterProScan 5:
645 genome-scale protein function classification. *Bioinform* **30**: 1236-1240.
646 Kapili, B.J., Barnett, S.E., Buckley, D.H., and Dekas, A.E. (2020) Evidence for phylogenetically
647 and catabolically diverse active diazotrophs in deep-sea sediment. *ISME J* **14**: 971-983.
648 Karl, D., Letelier, R., Tupas, L., Dore, J., Christian, J., and Hebel, D. (1997) The role of nitrogen
649 fixation in biogeochemical cycling in the subtropical North Pacific Ocean. *Nature* **388**: 533-
650 538.
651 Karsenti, E., Acinas, S.G., Bork, P., Bowler, C., De Vargas, C., Raes, J. et al. (2011) A Holistic
652 Approach to Marine Eco-Systems Biology. *Plos Biol* **9**.
653 Kelly, M.J.S., Poole, R.K., Yates, M.G., and Kennedy, C. (1990) Cloning and mutagenesis of
654 genes encoding the cytochrome-bd terminal oxidase complex in *Azotobacter vinelandii* -
655 mutants deficient in the cytochrome-D complex are unable to fix Nitrogen in air. *J Bacteriol*
656 **172**: 6010-6019.
657 Koster, J., and Rahmann, S. (2018) Snakemake-a scalable bioinformatics workflow engine.
658 *Bioinform* **34**: 3600.
659 Landolfi, A., Kahler, P., Koeve, W., and Oschlies, A. (2018) Global Marine N_2 Fixation
660 Estimates: From Observations to Models. *Front Microbiol* **9**: 2112.
661 Langmead, B., and Salzberg, S.L. (2012) Fast gapped-read alignment with Bowtie 2. *Nat*
662 *Methods* **9**: 357-359.
663 Le Roux, F., Binesse, J., Saulnier, D., and Mazel, D. (2007) Construction of a *Vibrio splendidus*
664 mutant lacking the metalloprotease gene *vsm* by use of a novel counterselectable suicide
665 vector. *Appl Environ Microbiol* **73**: 777-784.
666 Lee, M.D. (2019) GToTree: a user-friendly workflow for phylogenomics. *Bioinform* **35**: 4162-
667 4164.
668 Martinez-Perez, C., Mohr, W., Schwedt, A., Durschlag, J., Callbeck, C.M., Schunck, H. et al.
669 (2018) Metabolic versatility of a novel N_2 -fixing Alphaproteobacterium isolated from a
670 marine oxygen minimum zone. *Environ Microbiol* **20**: 755-768.
671 Martinez-Perez, C., Mohr, W., Loscher, C.R., Dekaezemacker, J., Littmann, S., Yilmaz, P. et al.
672 (2016) The small unicellular diazotrophic symbiont, UCYN-A, is a key player in the marine
673 nitrogen cycle. *Nat Microbiol* **1**: 16163.
674 Mills, M.M., Turk-Kubo, K.A., van Dijken, G.L., Henke, B.A., Harding, K., Wilson, S.T. et al.
675 (2020) Unusual marine *cyanobacteria*/haptophyte symbiosis relies on N_2 fixation even in N-
676 rich environments. *ISME J* **14**: 2395-2406.

Morot, A., El Fekih, S., Bidault, A., Le Ferrand, A., Jouault, A., Kavousi, J. et al. (2021) Virulence of *Vibrio harveyi* ORM4 towards the European abalone *Haliotis tuberculata* involves both quorum sensing and a type III secretion system. *Environ Microbiol* **23**: 5273-5288.

Mulholland, M.R., Bernhardt, P.W., Widner, B.N., Selden, C.R., Chappell, P.D., Clayton, S. et al. (2019) High rates of N_2 fixation in temperate, Western North Atlantic coastal waters expand the realm of marine diazotrophy. *Glob Biogeochem Cycles* **33**: 826-840.

Nieves-Morion, M., Flores, E., and Foster, R.A. (2020) Predicting substrate exchange in marine diatom-heterocystous cyanobacteria symbioses. *Environ Microbiol* **22**: 2027-2052.

Nieves-Morion, M., Flores, E., Whitehouse, M.J., Thomen, A., and Foster, R.A. (2021) Single-cell measurements of fixation and intercellular exchange of C and N in the filaments of the heterocyst-forming Cyanobacterium *Anabaena* sp. strain PCC 7120. *mBio* **12**: e0131421.

Pamp, S.J., Sternberg, C., and Tolker-Nielsen, T. (2009) Insight into the microbial multicellular lifestyle via flow-cell technology and confocal microscopy. *Cytometry A* **75**: 90-103.

Planes, S., Allemand, D., Agostini, S., Banaigs, B., Boissin, E., Boss, E. et al. (2019) The Tara Pacific expedition-A pan-ecosystemic approach of the "-omics" complexity of coral reef holobionts across the Pacific Ocean. *PLoS Biol* **17**: e3000483.

Poole, R.K., and Hill, S. (1997) Respiratory protection of nitrogenase activity in *Azotobacter vinelandii* - Roles of the terminal oxidases. *Biosci Rep* **17**: 303-317.

Price, M.N., Dehal, P.S., and Arkin, A.P. (2010) FastTree 2--approximately maximum-likelihood trees for large alignments. *PLoS One* **5**: e9490.

Sabra, W., Zeng, A.P., Lunsdorf, H., and Deckwer, W.D. (2000) Effect of oxygen on formation and structure of *Azotobacter vinelandii* alginate and its role in protecting nitrogenase. *Appl Environ Microbiol* **66**: 4037-4044.

Soree, M., Delavat, F., Lambert, C., Lozach, S., Papin, M., Petton, B. et al. (2022) Life-history of oysters influence *Vibrio parahaemolyticus* accumulation in Pacific oysters (*Crassostrea gigas*). *Environ Microbiol*.

Stewart, P.S., Zhang, T., Xu, R., Pitts, B., Walters, M.C., Roe, F. et al. (2016) Reaction-diffusion theory explains hypoxia and heterogeneous growth within microbial biofilms associated with chronic infections. *NPJ Biofilms Microbiomes* **2**: 16012.

Tamaki, H., Hanada, S., Sekiguchi, Y., Tanaka, Y., and Kamagata, Y. (2009) Effect of gelling agent on colony formation in solid cultivation of microbial community in lake sediment. *Environ Microbiol***11**: 1827-1834.

Tang, W., Wang, S., Fonseca-Batista, D., Dehairs, F., Gifford, S., Gonzalez, A.G. et al. (2019) Revisiting the distribution of oceanic N_2 fixation and estimating diazotrophic contribution to marine production. *Nat Commun* **10**: 831.

Tolker-Nielsen, T., and Sternberg, C. (2011) Growing and analyzing biofilms in flow chambers. *Curr Protoc Microbiol* **Chapter 1**: Unit 1B 2.

Tuit, C., Waterbury, J., and Ravizza, G. (2004) Diel variation of molybdenum and iron in marine diazotrophic cyanobacteria. *Limnol Oceanogr***49**: 978-990.

Wang, D., Xu, A., Elmerich, C., and Ma, L.Z. (2017) Biofilm formation enables free-living nitrogen-fixing rhizobacteria to fix nitrogen under aerobic conditions. *ISME J* **11**: 1602-1613.

Xu, J., Ericson, C.F., Lien, Y.W., Rutaganira, F.U.N., Eisenstein, F., Feldmuller, M. et al. (2022) Identification and structure of an extracellular contractile injection system from the marine bacterium *Algoriphagus machipongonensis*. *Nat Microbiol* **7**: 397-410.

722 Zehr, J.P., Mellon, M.T., and Zani, S. (1998) New nitrogen-fixing microorganisms detected in
723 oligotrophic oceans by amplification of Nitrogenase (*nifH*) genes. *Appl Environ Microbiol* **64**:
724 3444-3450.
725 Zhang, C.C., Laurent, S., Sakr, S., Peng, L., and Bedu, S. (2006) Heterocyst differentiation and
726 pattern formation in *Cyanobacteria*: a chorus of signals. *Mol Microbiol* **59**: 367-375.
727

728

729 **Figure legend**

730

731 *Figure 1*

732 Microscopy picture showing the obtention of *V. diazotrophicus* carrying the GFP-expressing
733 plasmid pFD086. Images were acquired from LB-grown overnight cultures.

734

735 *Figure 2*

736 Genetic and physiological characterization of the *V. diazotrophicus* NS1 and the Δ*nifH*
737 mutant. (A) Gel electrophoresis showing the deletion of *nifH* in *V. diazotrophicus* NS1 (lanes
738 2 and 4). (B) Generation time of *V. diazotrophicus* NS1 and derivative mutants. *V.*
739 *diazotrophicus* NS1 and *V. diazotrophicus* NS1 Δ*nifH* contained the pFD085 plasmid and *V.*
740 *diazotrophicus* NS1 compl-*nifH* corresponds to *V. diazotrophicus* NS1 Δ*nifH* containing
741 pFD120. A one-way ANOVA with Tukey test was done to compare the different mutants.
742 Depicted here are the mean+SEM of 4 replicates.

743

744 *Figure 3*

745 Soft-gellan assay demonstrating bacterial growth under appropriate microoxic conditions.
746 The "+" and "-" indicate the presence or absence of NH_4^+, respectively. White arrows
747 indicate the location of the growing ring. Note the absence of ring in the Δ*nifH* mutant and
748 in the presence of NH_4^+. Similar results were obtained using NO_3^- as a bioavailable inorganic
749 nitrogen source (see Figure S1).

750

751 *Figure 4*

752 Biofilm formation characteristics of *V. diazotrophicus* NS1. (A) Corrected biofilm formation in
753 *V. diazotrophicus* NS1 and derivative mutants in different media. *V. diazotrophicus* NS1 and
754 *V. diazotrophicus* NS1 Δ*nifH* contained the pFD085 plasmid and *V. diazotrophicus* NS1

755 compl-*nifH* corresponds to *V. diazotrophicus* NS1 Δ*nifH* containing pFD120. Presented here
756 are the mean+SEM of at least three replicates. Significance was assessed by one-way ANOVA
757 with Tukey test for each mutant in the different media. (B) View of the top of the biofilm
758 produced by *V. diazotrophicus* NS1 pFD086 after 24 hours of incubation in a flow cell. (C)
759 Stacked microsopy image showing the thickness of the biofilm produced after 24 hours. (D)
760 Average and maximal thickness of the biofilm produced by *V. diazotrophicus* NS1 pFD086
761 after 24 hours. See Figure S3 for images corresponding to timepoint 48 hours.
762
763 **Figure 5. Comparative genomics of *V. diazotrophicus* NS1.** (A) Phylogenomics tree of *V.*
764 *diazotrophicus* NS1 and the 40 diazotroph MAGs from (Delmont et al., 2022) using 16 single
765 copy core genes occurring in at least 40 of the 41 genomes. We used FastTree to compute a
766 phylogenomic tree and anvi'o (Eren et al., 2021) for the visualization. (B) Pangenomics
767 analysis of publicly available *V. diazotrophicus*. A total of 6,928 gene clusters are represented
768 in the figure with each darker color in the genome's layer indicating the presence of gene
769 cluster in the corresponding genome. The red selection highlights the 2,884 single-copy core
770 genes. The heatmap corresponds to the ANI computed between all genomes and it is scaled
771 from below 0.95 ANI (white) to 1 ANI (dark red). We generated a phylogenomics tree (shown
772 above the ANI heatmap) using a subset of set of 99 single copy core gene with a maximum
773 functional homogeneity of 0.95 using anvi'o. (C) Conserved synteny of the *nif* gene locus
774 across multiple *V. diazotrophicus* genomes. The scale is based on the total size of the locus in
775 *V. diazotrophicus* NS1. The double bars indicates that the locus continues on a different
776 contig. Acc. Num: 65.7M (POSL00000000), 65.10M (POSM00000000), 60.27F
777 (POSK00000000), 60.18M (POSJ00000000), 60.6F (POSI00000000), 60.6B (POSH00000000),
778 HF9B (JAATOR000000000) and 99A (PRJNA456207).
779
780 *Supplementary Figure S1*
781 Soft-gellan assay demonstrating bacterial growth under appropriate microoxic conditions.
782 The "+" and "-" indicate the presence or absence of NO_3^-, respectively. White arrows
783 indicate the location of the growing ring. Note the absence of ring in the Δ*nifH* mutant and
784 in the presence of NH_4^+.
785
786 *Supplementary Figure S2*

787 Microscopy picture of *V. diazotrophicus* NS1 pFD086 cells grown under microoxic condition
788 in a nitrogen-free MDV soft-gellan medium. Cells from the growing ring were pipetted with a
789 syringe and a needle, and observed by epifluorescence microscopy. Please note that cells are
790 isolated and don't form aggregates.
791
792 *Supplementary Figure S3*
793 (A) View of the top of the biofilm produced by *V. diazotrophicus* NS1 pFD086 after 48 hours
794 of incubation in a flow cell. (B) three-dimensional representation showing the thickness of
795 the biofilm produced after 48 hours.
796

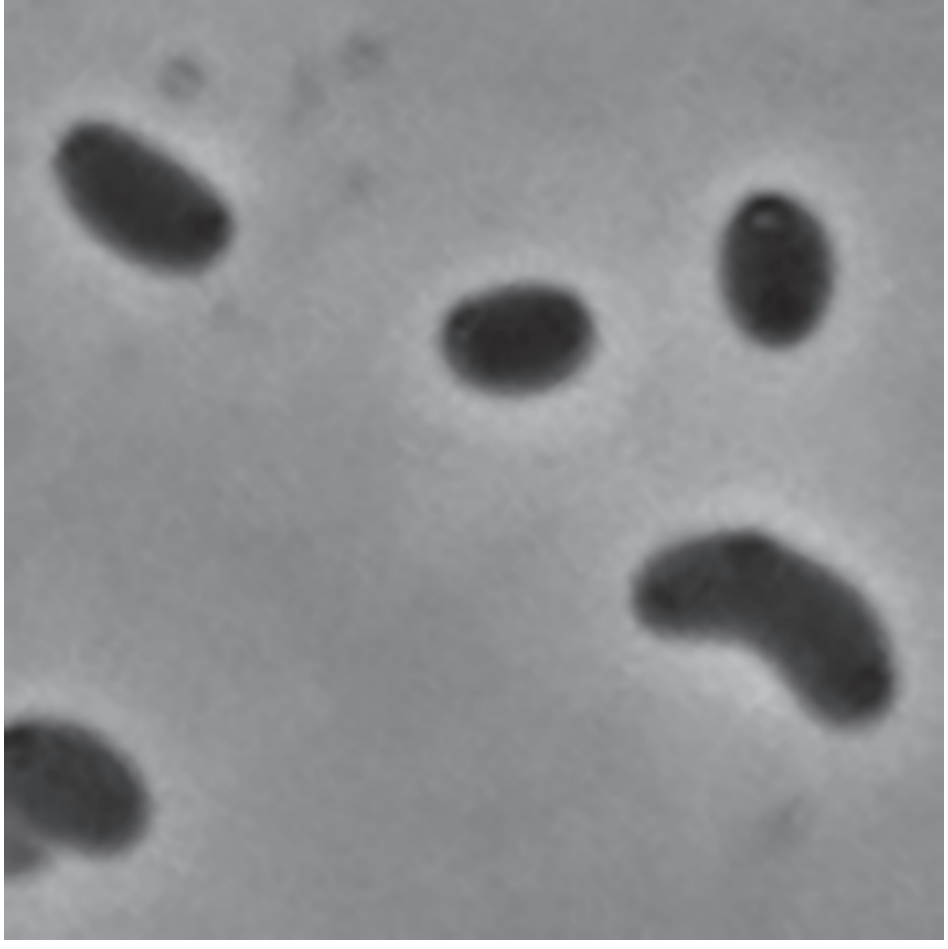

Phase Contrast

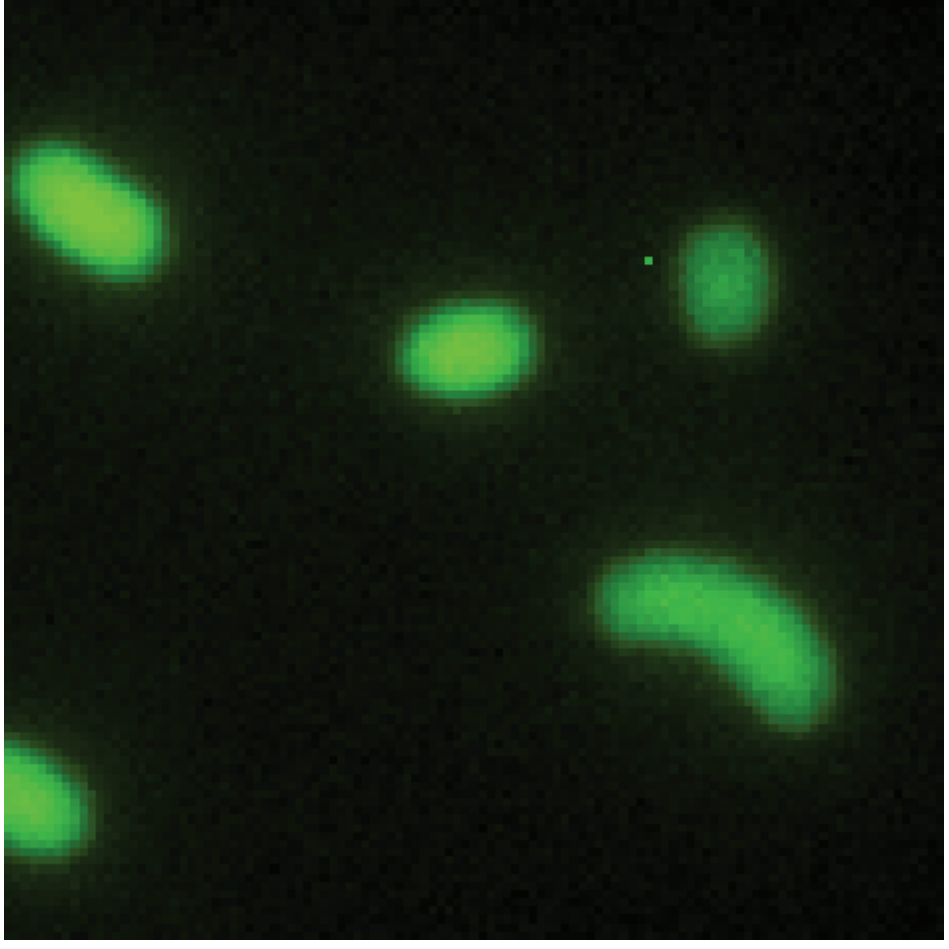

GFP

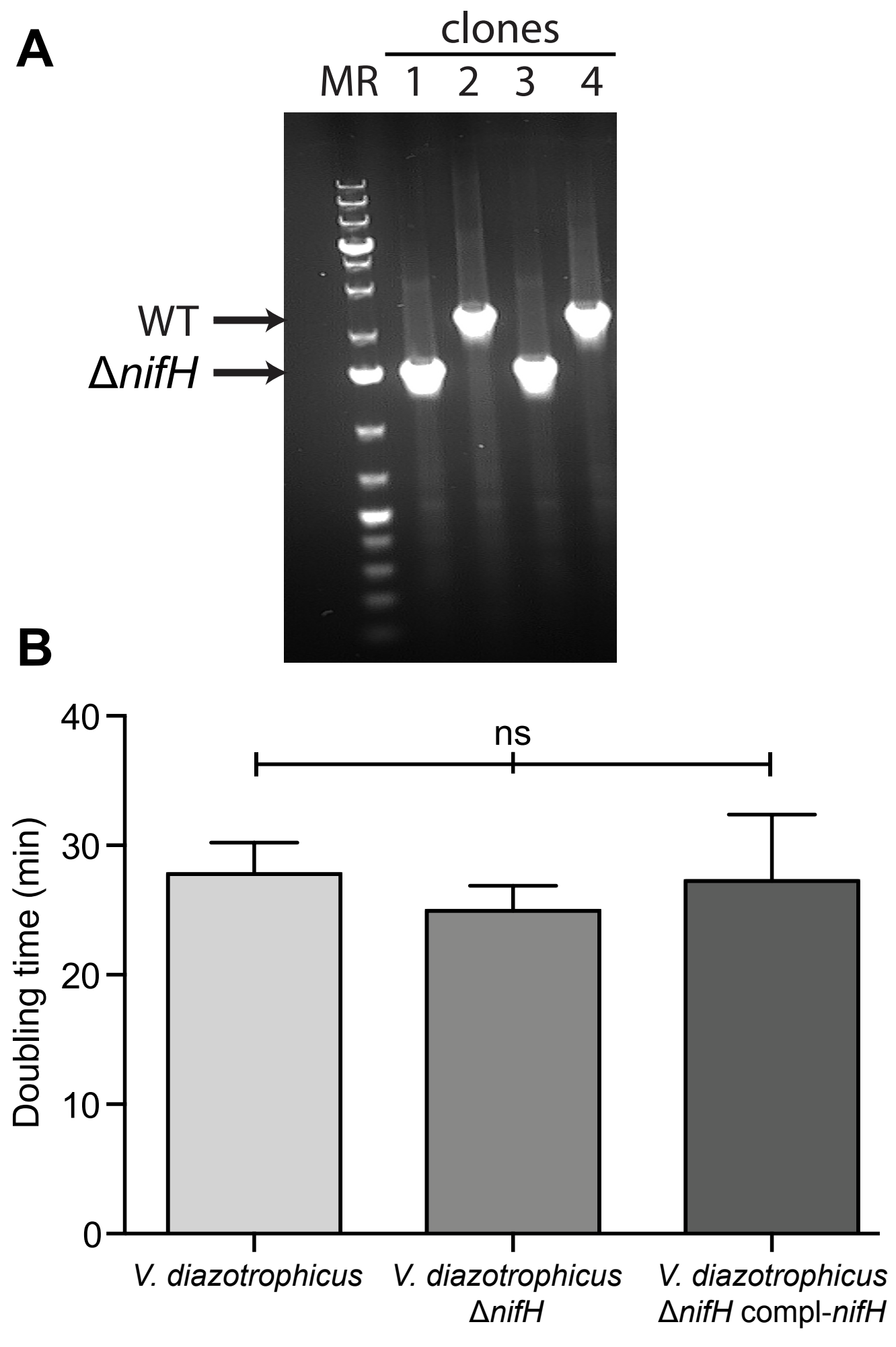
A
clones
MR
1
2
3
4
WT
ΔnifH
B
ns
Doubling time (min)
40
30
20
10
0
V. diazotrophicus
V. diazotrophicus ΔnifH
V. diazotrophicus ΔnifH compl-nifH

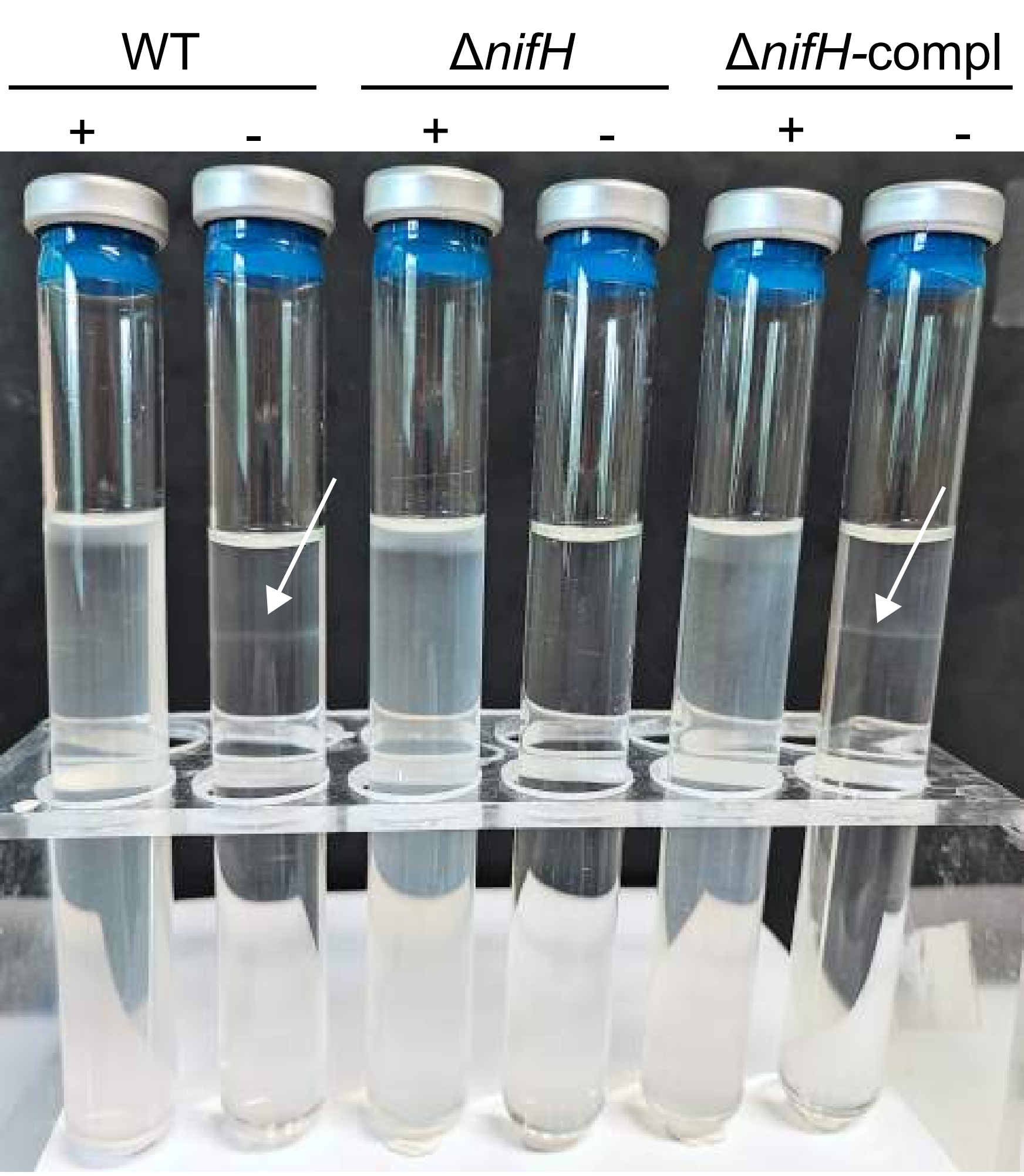
WT
Δ*nifH*
Δ*nifH*-compl
+
-
+
-
+
-

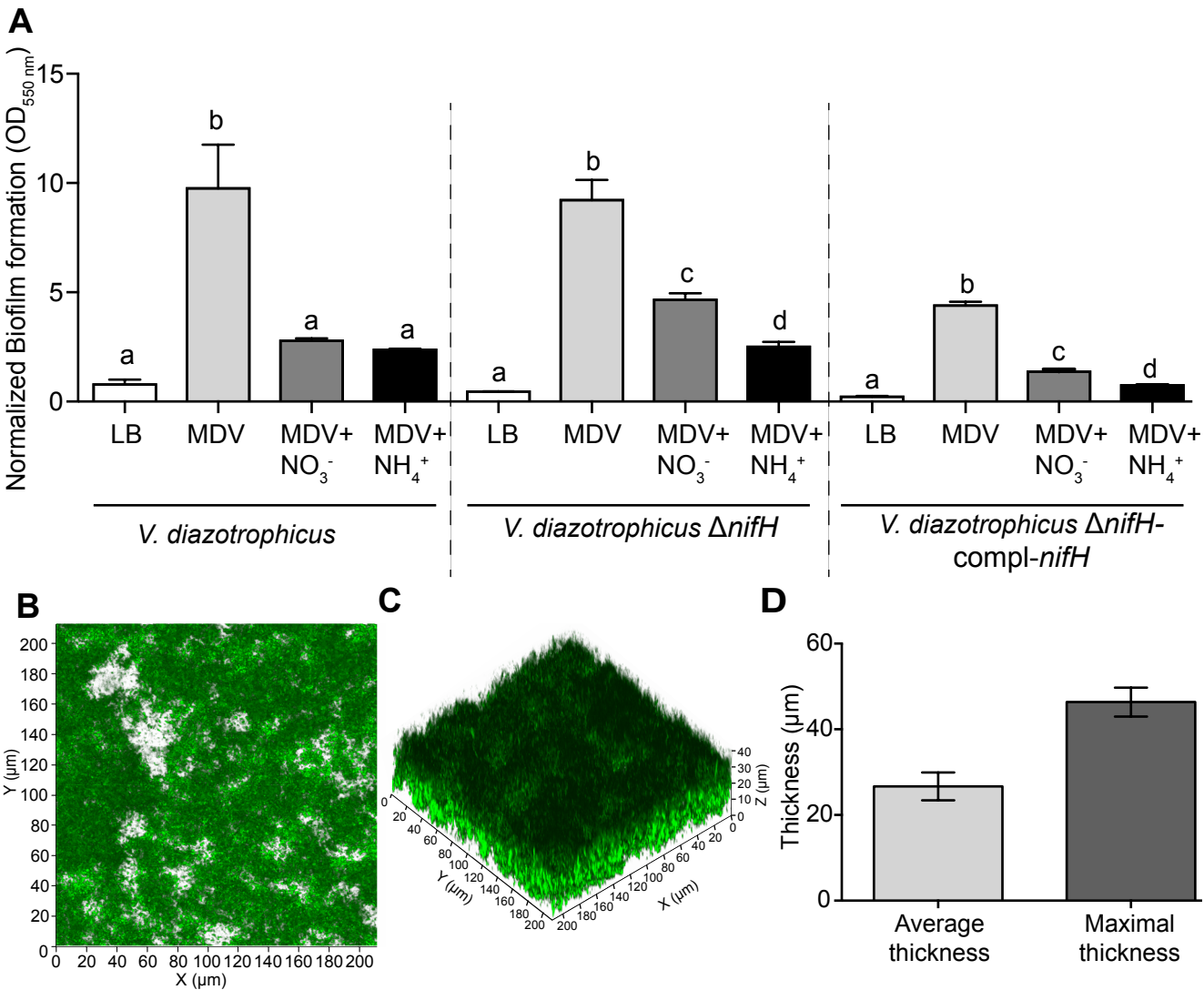
A
Normalized Biofilm formation ($OD_{550\ nm}$)
15
10
5
0
a
b
a
a
a
b
c
d
a
b
c
d
LB
MDV
MDV+ NO_3^-
MDV+ NH_4^+
LB
MDV
MDV+ NO_3^-
MDV+ NH_4^+
LB
MDV
MDV+ NO_3^-
MDV+ NH_4^+
V. diazotrophicus
V. diazotrophicus ΔnifH
V. diazotrophicus ΔnifH-compl-nifH
B
Y (µm)
X (µm)
C
Z (µm)
Y (µm)
X (µm)
D
Thickness (µm)
60
40
20
0
Average thickness
Maximal thickness

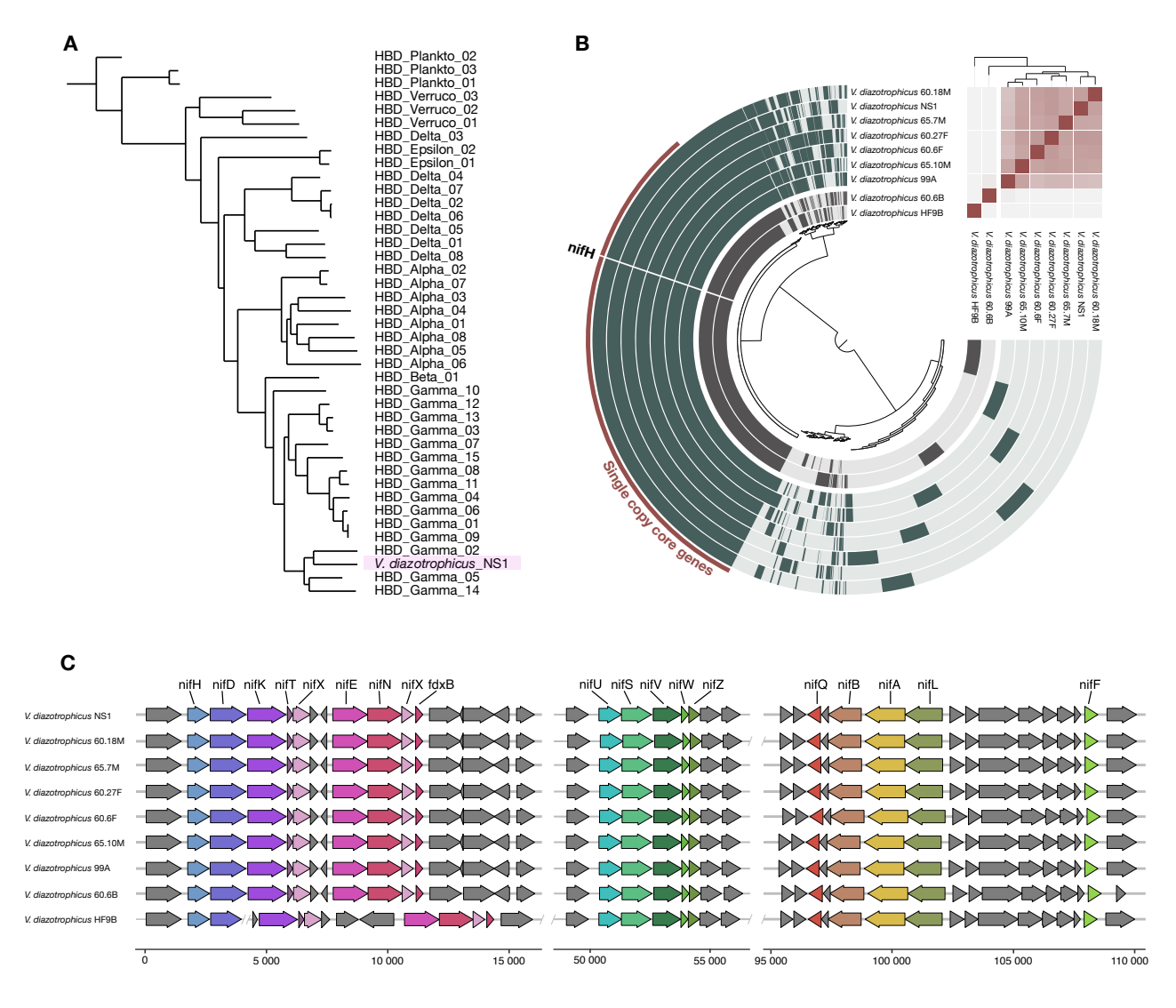
A
HBD_Plankto_02
HBD_Plankto_03
HBD_Plankto_01
HBD_Verruco_03
HBD_Verruco_02
HBD_Verruco_01
HBD_Delta_03
HBD_Epsilon_02
HBD_Epsilon_01
HBD_Delta_04
HBD_Delta_07
HBD_Delta_02
HBD_Delta_06
HBD_Delta_05
HBD_Delta_01
HBD_Delta_08
HBD_Alpha_02
HBD_Alpha_07
HBD_Alpha_03
HBD_Alpha_04
HBD_Alpha_01
HBD_Alpha_08
HBD_Alpha_05
HBD_Alpha_06
HBD_Beta_01
HBD_Gamma_10
HBD_Gamma_12
HBD_Gamma_13
HBD_Gamma_03
HBD_Gamma_07
HBD_Gamma_15
HBD_Gamma_08
HBD_Gamma_11
HBD_Gamma_04
HBD_Gamma_06
HBD_Gamma_01
HBD_Gamma_09
HBD_Gamma_02
V. diazotrophicus_NS1
HBD_Gamma_05
HBD_Gamma_14
B
V. diazotrophicus 60.18M
V. diazotrophicus NS1
V. diazotrophicus 65.7M
V. diazotrophicus 60.27F
V. diazotrophicus 60.6F
V. diazotrophicus 65.10M
V. diazotrophicus 99A
V. diazotrophicus 60.6B
V. diazotrophicus HF9B
nifH
Single copy core genes
C
nifH
nifD
nifK
nifT
nifX
nifE
nifN
nifX
fdxB
nifU
nifS
nifV
nifW
nifZ
nifQ
nifB
nifA
nifL
nifF
V. diazotrophicus NS1
V. diazotrophicus 60.18M
V. diazotrophicus 65.7M
V. diazotrophicus 60.27F
V. diazotrophicus 60.6F
V. diazotrophicus 65.10M
V. diazotrophicus 99A
V. diazotrophicus 60.6B
V. diazotrophicus HF9B
0
5 000
10 000
15 000
50 000
55 000
95 000
100 000
105 000
110 000